

EVALUATION OF  $n + {}^{28}\text{Si}$  CROSS SECTIONS FOR THE ENERGY  
RANGE  $1.0\text{E-}11$  to  $150\text{ MeV}$

M. B. Chadwick and P. G. Young  
1 July 1997

This evaluation provides a complete representation of the nuclear data needed for transport, damage, heating, radioactivity, and shielding applications over the incident neutron energy range from  $1.0\text{E-}11$  to  $150\text{ MeV}$ . The discussion here is divided into the region below and above  $20\text{ MeV}$ .

INCIDENT NEUTRON ENERGIES  $< 20\text{ MeV}$

Below  $20\text{ MeV}$  the evaluation is based completely on the ENDF/B-VI.5 (Release 5) evaluation by D. Hetrick, N. Larson, D. Larson, L. Leal, and S. Epperson.

INCIDENT NEUTRON ENERGIES  $> 20\text{ MeV}$

The ENDF/B-VI Release 5 evaluation extends to  $20\text{ MeV}$  and includes cross sections and energy-angle data for all significant reactions. The present evaluation utilizes a more compact composite reaction spectrum representation above  $20\text{ MeV}$  in order to reduce the length of the file. No essential data for applications is lost with this representation.

The evaluation above  $20\text{ MeV}$  utilizes MF=6, MT=5 to represent all reaction data. Production cross sections and emission spectra are given for neutrons, protons, deuterons, tritons, alpha particles, gamma rays, and all residual nuclides produced ( $A > 5$ ) in the reaction chains. To summarize, the ENDF sections with non-zero data above  $E_n = 20\text{ MeV}$  are:

MF=3	MT= 1	Total Cross Section
	MT= 2	Elastic Scattering Cross Section
	MT= 3	Nonelastic Cross Section
	MT= 5	Sum of Binary $(n,n')$ and $(n,x)$ Reactions
MF=4	MT= 2	Elastic Angular Distributions
MF=6	MT= 5	Production Cross Sections and Energy-Angle Distributions for Emission Neutrons, Protons, Deuterons, Tritons, and Alphas; and Angle-Integrated Spectra for Gamma Rays and Residual

Nuclei That Are Stable Against Particle Emission

The evaluation is based on nuclear model calculations that have been benchmarked to experimental data, especially for  $n + {}^{28}\text{Si}$  and  $p + {}^{28}\text{Si}$  reactions (Ch97). We use the GNASH code system (Yo92), which utilizes Hauser-Feshbach statistical, preequilibrium and direct-reaction theories. Spherical optical model calculations are used to obtain particle transmission coefficients for the Hauser-Feshbach calculations, as well as for the elastic neutron angular distributions.

Cross sections and spectra for producing individual residual nuclei are included for reactions. The energy-angle-correlations for all outgoing particles are based on Kalbach systematics (Ka88).

A model was developed to calculate the energy distributions of all recoil nuclei in the GNASH calculations (Ch96). The recoil energy distributions are represented in the laboratory system in MT=5, MF=6, and are given as isotropic in the lab system. All other data in MT=5, MF=6 are given in the center-of-mass system. This method of representation utilizes the LCT=3 option approved at the November, 1996, CSEWG meeting.

Preequilibrium corrections were performed in the course of the GNASH calculations using the exciton model of Kalbach (Ka77, Ka85), validated by comparison with calculations using Feshbach, Kerman, Koonin (FKK) theory [Ch93]. Discrete level data from nuclear data sheets were matched to continuum level densities using the formulation of Ignatyuk (Ig75) and pairing and shell parameters from the Cook (Co67) analysis. Neutron and charged-particle transmission coefficients were obtained from the optical potentials, as discussed below. Gamma-ray transmission coefficients were calculated using the Kopecky-Uhl model (Ko90).

#### DETAILS OF THE n + SI-28 ANALYSIS

The neutron total cross section above 20 MeV was obtained by evaluating the experimental data, with a particular emphasis on the high-accuracy Los Alamos measurements by Finlay (Fi93).

The Madland global medium-energy optical potential (Ma88) was used for neutrons above 46 MeV, and the Wilmore-Hodgson potential [Wi64] was used for lower neutron energies. The Madland global medium-energy optical potential was used for protons above 28 MeV, and the Becchetti-Greenlees potential [Be69] was used for lower proton energies. In both cases the transition region to the Madland potential was chosen to approximately give continuity in the reaction cross section. For deuterons, the Perey [Pe63] global potential was used; for alpha particles the MacFadden potential [Ma66] was used; and for tritons the Becchetti-Greenlees potential [Be71] was used.

While the above optical potentials did describe the experimental proton nonelastic cross section data fairly well, we modified the theoretical predictions slightly to better agree with the measurements, and renormalized the transmission coefficients accordingly. In addition to using Si nonelastic proton cross section measurements, we also were guided by p+Al nonelastic data, scaled by  $A^{2/3}$ .

Coupled-channel optical model calculations were performed to determine inelastic scattering on  $^{28}\text{Si}$ , for the  $0^+$ ,  $2^+$ , and  $4^+$  states, as well as a DWBA calculation of the inelastic scattering to the 3- vibrational state, all performed with the ECIS code [Ra72]. Near 20 MeV neutron energy, inelastic scattering to these states has been measured by Alarcon and Rapaport [Al83], and Finlay et al., from Ohio University, and the inelastic cross sections to these collective states is in good agreement with the ORNL ENDF evaluation for  $^{28}\text{Si}$ . To produce continuity in the calculated inelastic cross sections up to 150 MeV, we performed a rotational band ( $0^+$ ,  $2^+$ ,  $4^+$ ) coupled channel calculation using the Madland medium energy potential (with its imaginary potential reduced by 20%, to approximately account for the coupling). Deformation parameters were chosen to reproduce the ENDF/B-VI cross sections at 20 MeV, resulting in values of  $\beta_{20} = -0.365$ ,  $\beta_{40} = +0.22$ , in good agreement with

Rapaport's values of -0.37, 0.17 respectively. A vibrational DWBA calculation (using ECIS) was performed for the 3- state resulting in  $\beta_3=0.235$  (Rapaport obtained 0.23).

Only 2 measurements exist for neutron-induced emission spectra above 20 MeV for  $^{28}\text{Si}$ . New data have been published by the Louvain group at the 1997 Trieste conference for 63 MeV  $\text{Si}(n,x\gamma)$

double-differential spectra ( $z=p,d,\alpha$  ejectiles). Additionally, Haight et al. of Los Alamos have preliminary data for  $\text{Si}(n,xp)$ , for neutrons up to 50 MeV, including emission spectra at four angles. Our calculations agree reasonably well with these measurements. While default level density parameters (using the Ignatyuk model) were utilized, in the case of  $^{28}\text{Al}$  the level density parameter was slightly modified to optimize agreement with the Abfalterer total level density measurements based on fluctuation analyses (Ab93).

As an independent validation of our GNASH calculations using the exciton model, we have also performed FKK calculations. This was done by implementing a multistep reaction theory recently developed by Koning and Chadwick, which is particularly suited to the simultaneous calculation of neutron and proton emission. The FKK theory describes the forward-peaking very well, as do our exciton model calculations using the phenomenological Kalbach angular distribution systematics.

\*\*\*\*\*

#### REFERENCES

- [Ab93] W. Abfalterer, R.W. Finlay, S.M. Grimes, and V. Mishra, Phys. Rev. C47, 1033 (1993).
- [Al83] R. Alarcon and J. Rapaport, Nucl. Phys. A458, 502 (1986).
- [Be69]. F.D. Becchetti, Jr., and G.W. Greenlees, Phys. Rev. 182, 1190 (1969).
- [Be71]. F.D. Becchetti, Jr., and G.W. Greenlees in "Polarization Phenomena in Nuclear Reactions," (Ed: H.H. Barschall and W. Haeberli, The University of Wisconsin Press, 1971) p.682.
- [Ch93]. M. B. Chadwick and P. G. Young, "Feshbach-Kerman-Koonin Analysis of  $^{93}\text{Nb}$  Reactions: P  $\rightarrow$  Q Transitions and Reduced Importance of Multistep Compound Emission," Phys. Rev. C 47, 2255 (1993).
- [Ch96]. M. B. Chadwick, P. G. Young, R. E. MacFarlane, and A. J. Koning, "High-Energy Nuclear Data Libraries for Accelerator-Driven Technologies: Calculational Method for Heavy Recoils," Proc. of 2nd Int. Conf. on Accelerator Driven Transmutation Technology and Applications, Kalmar, Sweden, 3-7 June 1996.
- [Ch97]. M. B. Chadwick and P. G. Young, "GNASH Calculations of  $n,p + \text{Si}$  isotopes and Benchmarking of Results" in APT PROGRESS REPORT: 1 June - 1 July 1997, internal Los Alamos National Laboratory memo T-2-97/MS-43, 7 July 1997 from R.E. MacFarlane to L. Waters.

- [Co67]. J. L. Cook, H. Ferguson, and A. R. Musgrove, "Nuclear Level Densities in Intermediate and Heavy Nuclei," Aust.J.Phys. 20, 477 (1967).
- [Fi93]. R. W. Finlay, W. P. Abfalterer, G. Fink, E. Montei, T. Adami, P. W. Lisowski, G. L. Morgan, and R. C. Haight, Phys. Rev. C 47, 237 (1993).
- [Ig75]. A. V. Ignatyuk, G. N. Smirenkin, and A. S. Tishin, "Phenomenological Description of the Energy Dependence of the Level Density Parameter," Sov. J. Nucl. Phys. 21, 255 (1975).
- [Ka77]. C. Kalbach, "The Griffin Model, Complex Particles and Direct Nuclear Reactions," Z.Phys.A 283, 401 (1977).
- [Ka85]. C. Kalbach, "PRECO-D2: Program for Calculating Preequilibrium and Direct Reaction Double Differential Cross Sections," Los Alamos National Laboratory report LA-10248-MS (1985).
- [Ka88]. C. Kalbach, "Systematics of Continuum Angular Distributions: Extensions to Higher Energies," Phys.Rev.C 37, 2350 (1988); see also C. Kalbach and F. M. Mann, "Phenomenology of Continuum Angular Distributions. I. Systematics and Parameterization," Phys.Rev.C 23, 112 (1981).
- [Ko90]. J. Kopecky and M. Uhl, "Test of Gamma-Ray Strength Functions in Nuclear Reaction Model Calculations," Phys.Rev.C 42, 1941 (1990).
- [Ma66]. L. MacFadden and G. R. Satchler, Nucl. Phys. 84, 177 (1966).
- [Ma88]. D.G. Madland, "Recent Results in the Development of a Global Medium-Energy Nucleon-Nucleus Optical-Model Potential," Proc. OECD/NEANDC Specialist's Mtg. on Preequilibrium Nuclear Reactions, Semmering, Austria, 10-12 Feb. 1988, NEANDC-245 'U' (1988).
- [Pe63]. C. M. Perey and F. G. Perey, Phys. Rev. 132, 755 (1963).
- [Ra72]. J. Raynal, "Optical Model and Coupled-Channels Calculations in Nuclear Physics", International Atomic Energy Agency report IAEA SMR-9/8, p. 281, Vienna (1972).
- [Wi64]. D. Wilmore and P. E. Hodgson, "The Calculation of Neutron Cross Sections from Optical Potentials," Nucl. Phys. 55, 673 (1964).
- [Yo92]. P. G. Young, E. D. Arthur, and M. B. Chadwick, "Comprehensive Nuclear Model Calculations: Introduction to the Theory and Use of the GNASH Code," LA-12343-MS (1992).

14028 = TARGET 1000Z+A (if A=0 then elemental)

1 = PROJECTILE 1000Z+A

Nonelastic, elastic, and Production cross sections for A&lt;5 ejectiles in barns:

Energy	nonelas	elastic	neutron	proton	deuteron	triton	helium3	alpha	gamma
2.000E+01	9.275E-01	9.125E-01	7.809E-01	3.991E-01	4.204E-02	4.389E-04	0.000E+00	1.626E-01	1.044E+00
2.200E+01	8.933E-01	9.867E-01	7.779E-01	4.033E-01	4.764E-02	1.039E-03	0.000E+00	1.611E-01	1.019E+00
2.400E+01	8.612E-01	1.045E+00	7.599E-01	4.123E-01	5.403E-02	1.620E-03	0.000E+00	1.575E-01	1.013E+00
2.600E+01	8.304E-01	1.095E+00	7.358E-01	4.149E-01	5.820E-02	1.838E-03	0.000E+00	1.691E-01	1.005E+00
2.800E+01	8.010E-01	1.133E+00	7.105E-01	4.323E-01	6.285E-02	2.337E-03	0.000E+00	1.608E-01	9.940E-01
3.000E+01	7.732E-01	1.164E+00	6.929E-01	4.520E-01	6.644E-02	2.814E-03	0.000E+00	1.572E-01	9.540E-01
3.500E+01	7.113E-01	1.217E+00	6.646E-01	4.913E-01	7.034E-02	4.481E-03	0.000E+00	1.499E-01	8.873E-01
4.000E+01	6.593E-01	1.232E+00	6.494E-01	5.153E-01	7.047E-02	6.093E-03	0.000E+00	1.436E-01	8.492E-01
4.500E+01	6.046E-01	1.228E+00	6.320E-01	5.203E-01	6.869E-02	7.459E-03	0.000E+00	1.498E-01	7.926E-01
5.000E+01	5.074E-01	1.191E+00	6.425E-01	5.424E-01	6.809E-02	8.417E-03	0.000E+00	1.451E-01	7.552E-01
5.500E+01	5.558E-01	1.130E+00	6.642E-01	5.663E-01	6.992E-02	9.335E-03	0.000E+00	1.472E-01	7.364E-01
6.000E+01	5.381E-01	1.062E+00	6.799E-01	5.878E-01	7.081E-02	1.036E-02	0.000E+00	1.575E-01	7.094E-01
6.500E+01	5.221E-01	9.959E-01	6.954E-01	6.067E-01	7.076E-02	1.116E-02	0.000E+00	1.587E-01	6.914E-01
7.000E+01	5.074E-01	9.346E-01	7.028E-01	6.190E-01	7.261E-02	1.216E-02	0.000E+00	1.612E-01	6.674E-01
7.500E+01	4.940E-01	8.680E-01	7.135E-01	6.344E-01	7.389E-02	1.310E-02	0.000E+00	1.645E-01	6.478E-01
8.000E+01	4.817E-01	8.073E-01	7.263E-01	6.443E-01	7.478E-02	1.416E-02	0.000E+00	1.690E-01	6.214E-01
8.500E+01	4.704E-01	7.466E-01	7.354E-01	6.499E-01	7.541E-02	1.472E-02	0.000E+00	1.678E-01	6.104E-01
9.000E+01	4.603E-01	6.967E-01	7.447E-01	6.647E-01	7.541E-02	1.595E-02	0.000E+00	1.729E-01	5.905E-01
9.500E+01	4.510E-01	6.470E-01	7.513E-01	6.703E-01	7.696E-02	1.704E-02	0.000E+00	1.758E-01	5.773E-01
1.000E+02	4.429E-01	6.021E-01	7.581E-01	6.798E-01	7.857E-02	1.824E-02	0.000E+00	1.766E-01	5.662E-01
1.100E+02	4.296E-01	5.264E-01	7.768E-01	6.962E-01	8.170E-02	2.066E-02	0.000E+00	1.821E-01	5.343E-01
1.200E+02	4.205E-01	4.606E-01	8.014E-01	7.206E-01	8.407E-02	2.343E-02	0.000E+00	1.872E-01	5.128E-01
1.300E+02	4.160E-01	4.030E-01	8.229E-01	7.447E-01	8.826E-02	2.624E-02	0.000E+00	1.887E-01	5.061E-01
1.400E+02	4.150E-01	3.530E-01	8.552E-01	7.727E-01	9.241E-02	2.934E-02	0.000E+00	1.933E-01	4.918E-01
1.500E+02	4.177E-01	3.103E-01	8.922E-01	8.090E-01	9.710E-02	3.281E-02	0.000E+00	1.995E-01	4.863E-01

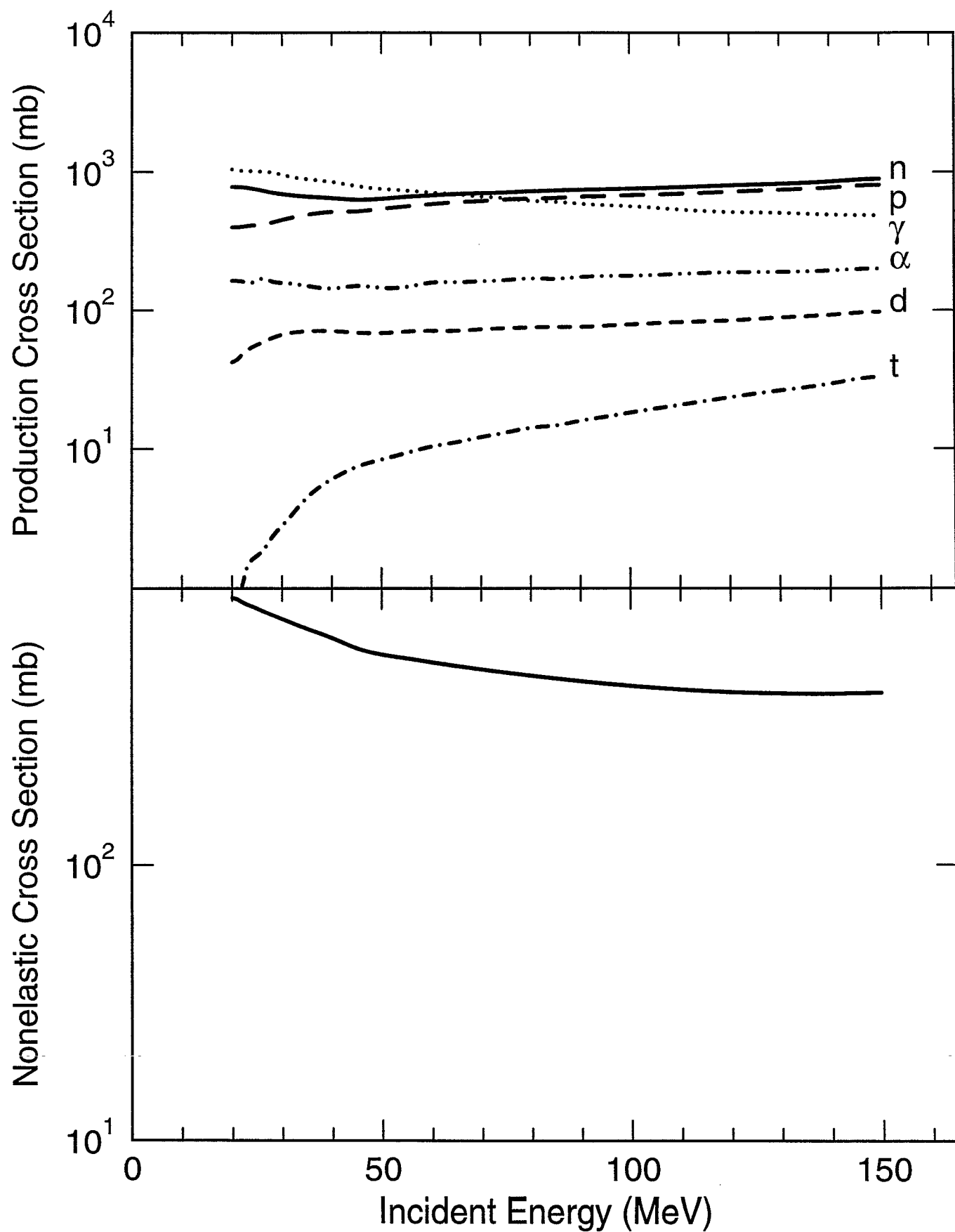
14028 = TARGET 1000Z+A (if A=0 then elemental)

1 = PROJECTILE 1000Z+A

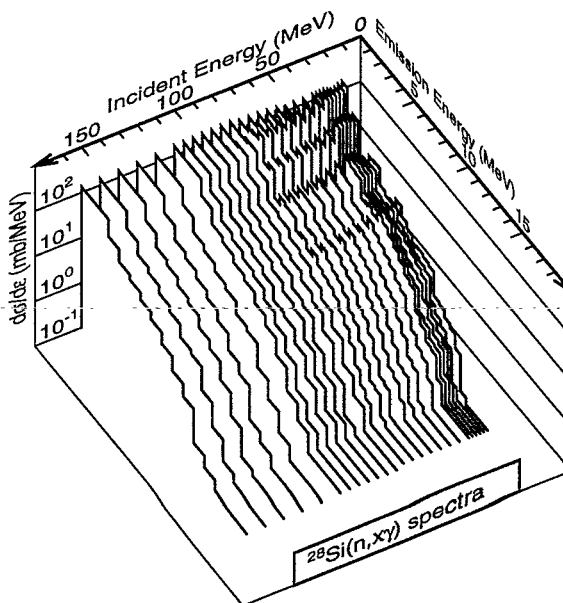
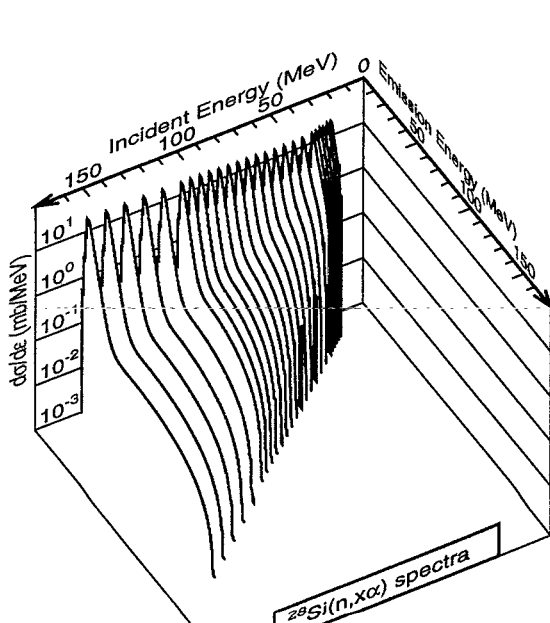
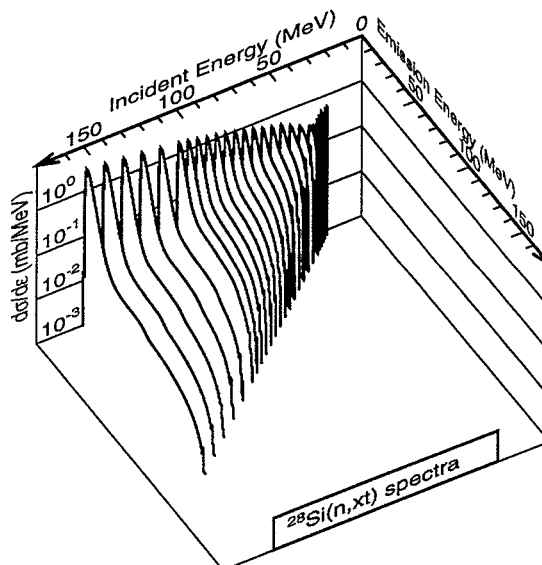
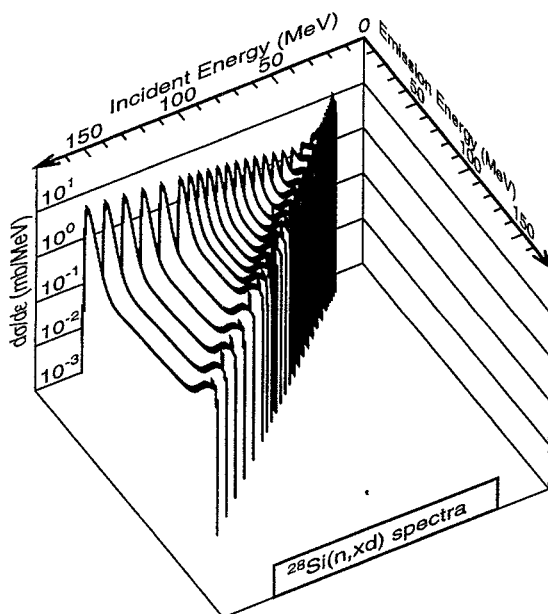
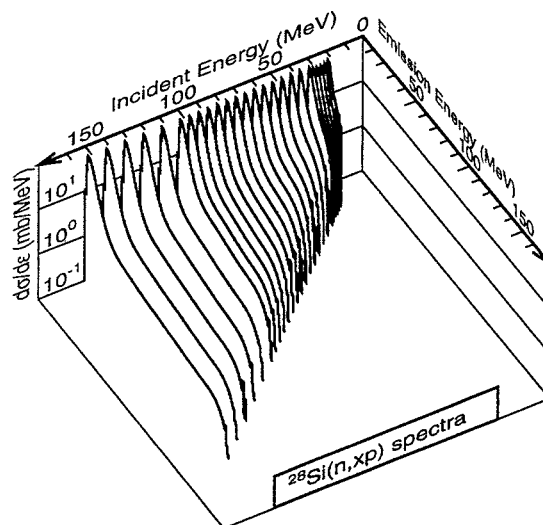
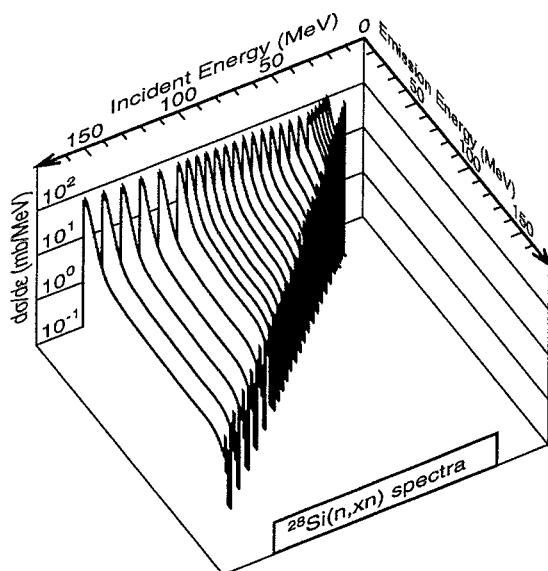
Kerma coefficients in units of f.Gy.m^2:

Energy	proton	deuteron	triton	helium3	alpha	non-rec	elas-rec	TOTAL
2.000E+01	6.499E-01	9.151E-02	3.779E-04	0.000E+00	3.496E-01	2.839E-01	7.872E-02	1.454E+00
2.200E+01	7.252E-01	1.249E-01	1.236E-03	0.000E+00	3.683E-01	2.950E-01	9.139E-02	1.606E+00
2.400E+01	7.997E-01	1.647E-01	2.436E-03	0.000E+00	3.771E-01	3.027E-01	9.127E-02	1.738E+00
2.600E+01	8.480E-01	2.005E-01	3.352E-03	0.000E+00	4.208E-01	3.070E-01	9.018E-02	1.870E+00
2.800E+01	9.307E-01	2.426E-01	5.029E-03	0.000E+00	4.228E-01	3.107E-01	8.826E-02	2.000E+00
3.000E+01	1.018E+00	2.837E-01	6.763E-03	0.000E+00	4.280E-01	3.139E-01	8.600E-02	2.137E+00
3.500E+01	1.208E+00	3.695E-01	1.317E-02	0.000E+00	4.329E-01	3.258E-01	7.996E-02	2.429E+00
4.000E+01	1.406E+00	4.450E-01	2.038E-02	0.000E+00	4.326E-01	3.333E-01	7.337E-02	2.711E+00
4.500E+01	1.543E+00	5.061E-01	2.707E-02	0.000E+00	4.660E-01	3.386E-01	6.748E-02	2.948E+00
5.000E+01	1.731E+00	5.652E-01	3.362E-02	0.000E+00	4.648E-01	3.448E-01	7.899E-02	3.218E+00
5.500E+01	1.948E+00	6.468E-01	3.997E-02	0.000E+00	4.757E-01	3.561E-01	7.092E-02	3.537E+00
6.000E+01	2.144E+00	7.176E-01	4.570E-02	0.000E+00	5.153E-01	3.689E-01	6.383E-02	3.855E+00
6.500E+01	2.345E+00	7.708E-01	5.134E-02	0.000E+00	5.249E-01	3.750E-01	5.786E-02	4.125E+00
7.000E+01	2.528E+00	8.511E-01	5.710E-02	0.000E+00	5.378E-01	3.829E-01	5.285E-02	4.410E+00
7.500E+01	2.717E+00	9.210E-01	6.253E-02	0.000E+00	5.498E-01	3.884E-01	4.804E-02	4.686E+00
8.000E+01	2.896E+00	9.777E-01	6.804E-02	0.000E+00	5.689E-01	3.945E-01	4.390E-02	4.949E+00
8.500E+01	3.076E+00	1.034E+00	7.206E-02	0.000E+00	5.696E-01	3.957E-01	4.002E-02	5.188E+00
9.000E+01	3.274E+00	1.062E+00	7.754E-02	0.000E+00	5.903E-01	3.941E-01	3.691E-02	5.434E+00
9.500E+01	3.447E+00	1.130E+00	8.184E-02	0.000E+00	6.035E-01	3.973E-01	3.394E-02	5.693E+00
1.000E+02	3.626E+00	1.195E+00	8.638E-02	0.000E+00	6.128E-01	4.000E-01	3.132E-02	5.952E+00
1.100E+02	3.993E+00	1.316E+00	9.517E-02	0.000E+00	6.405E-01	4.067E-01	2.702E-02	6.479E+00
1.200E+02	4.404E+00	1.395E+00	1.051E-01	0.000E+00	6.704E-01	4.081E-01	2.338E-02	7.007E+00
1.300E+02	4.836E+00	1.535E+00	1.145E-01	0.000E+00	6.908E-01	4.286E-01	2.027E-02	7.626E+00
1.400E+02	5.307E+00	1.647E+00	1.251E-01	0.000E+00	7.183E-01	4.558E-01	1.759E-02	8.271E+00
1.500E+02	5.852E+00	1.766E+00	1.375E-01	0.000E+00	7.539E-01	4.796E-01	1.531E-02	9.004E+00

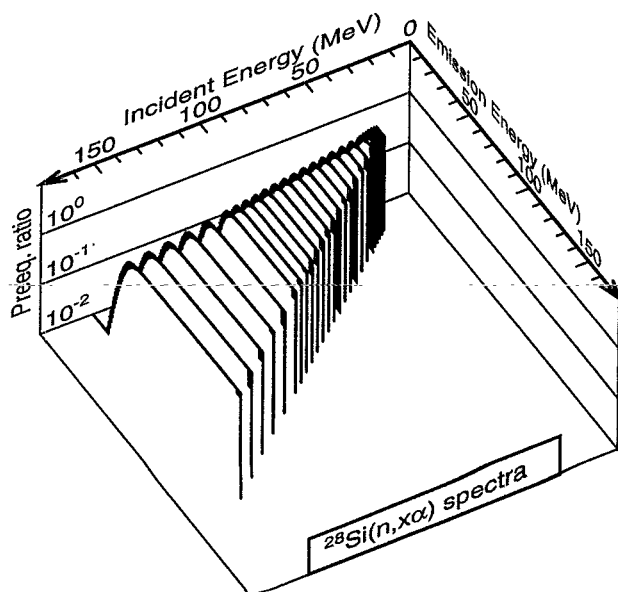
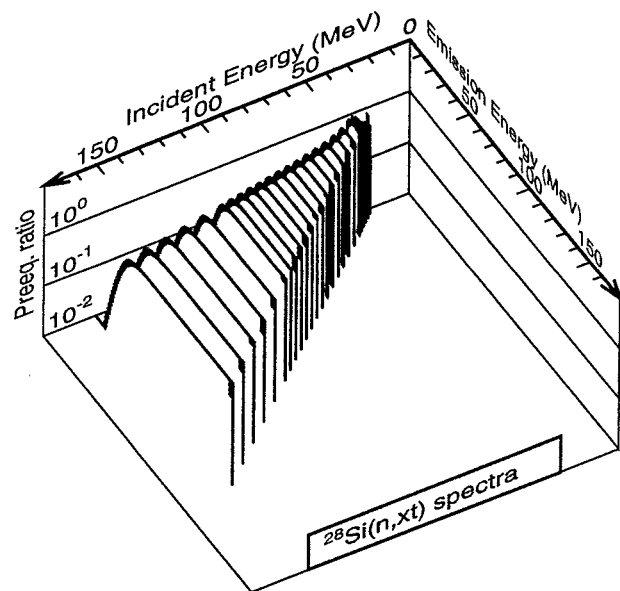
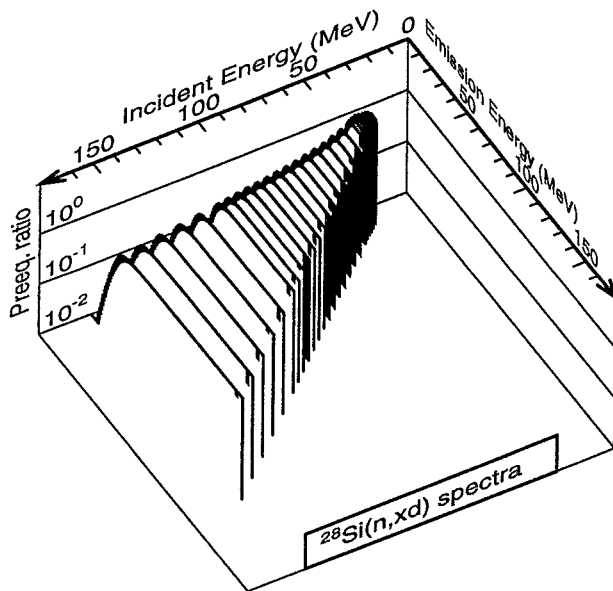
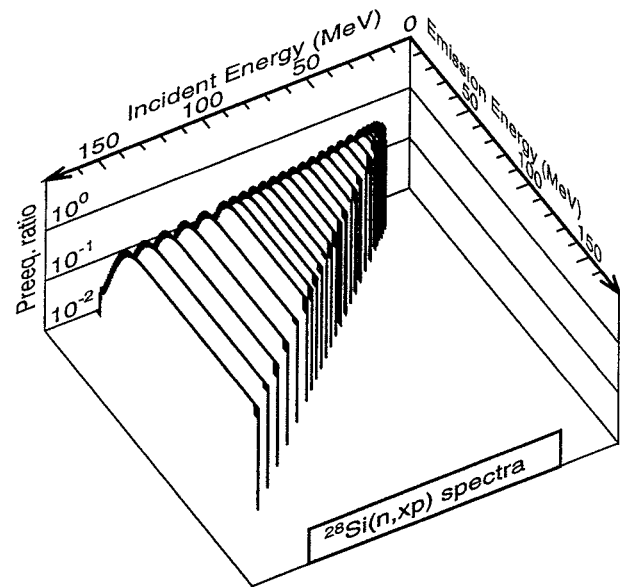
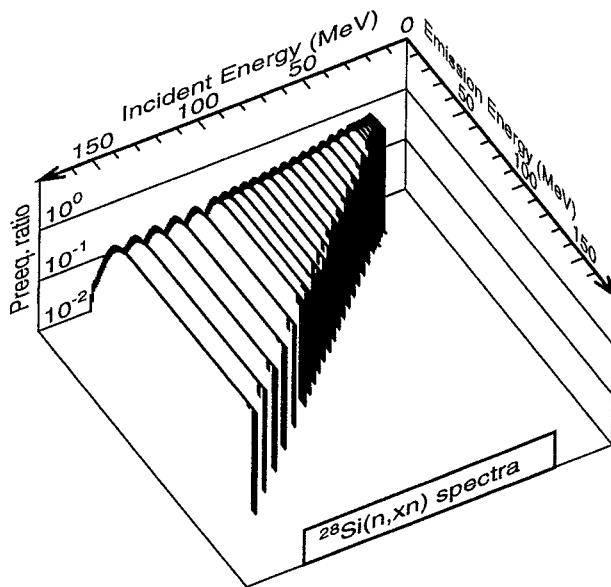
$n + {}^{28}\text{Si}$  nonelastic and production cross sections



# $n + {}^{28}\text{Si}$ angle-integrated emission spectra

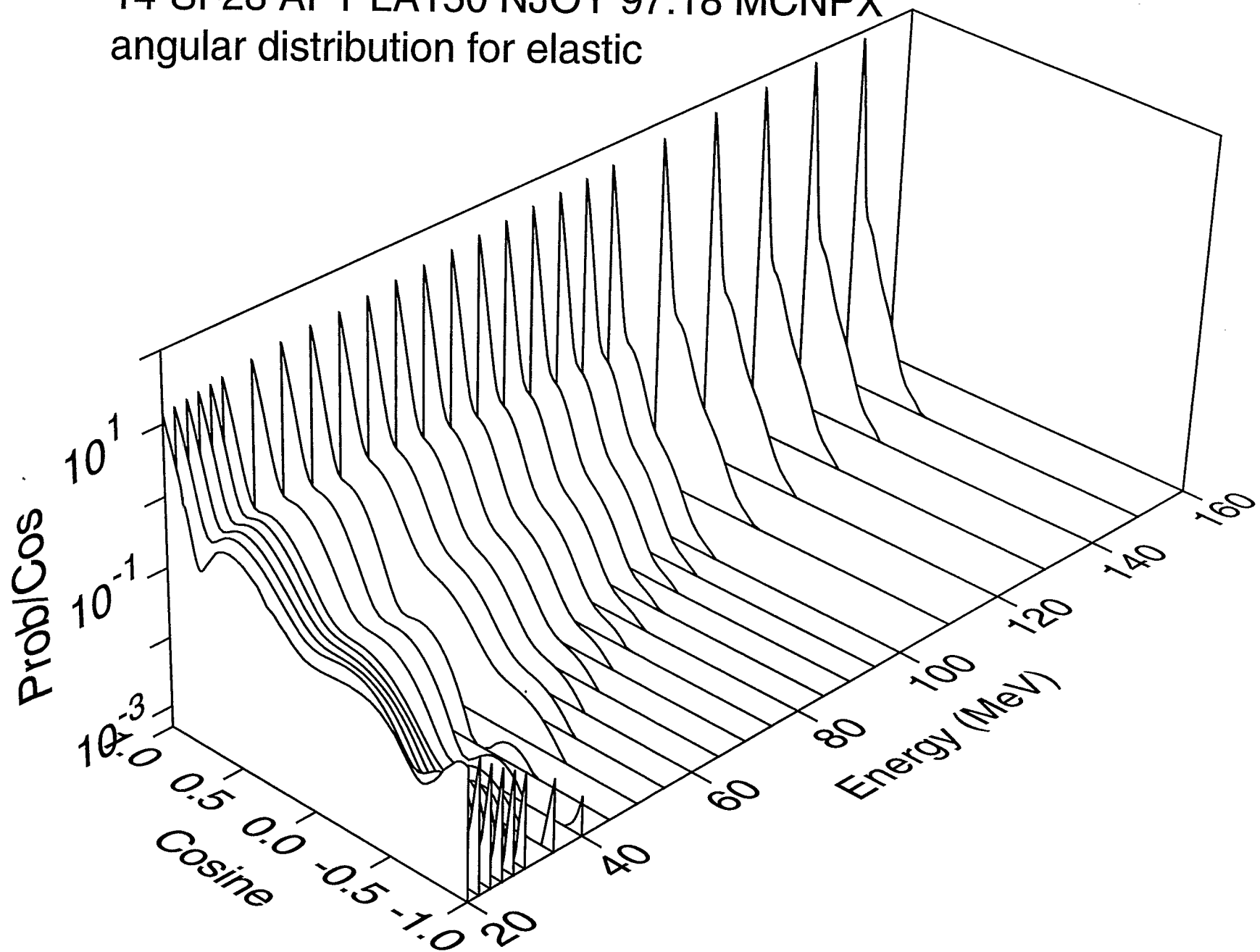


# $n + {}^{28}\text{Si}$ Kalbach preequilibrium ratios



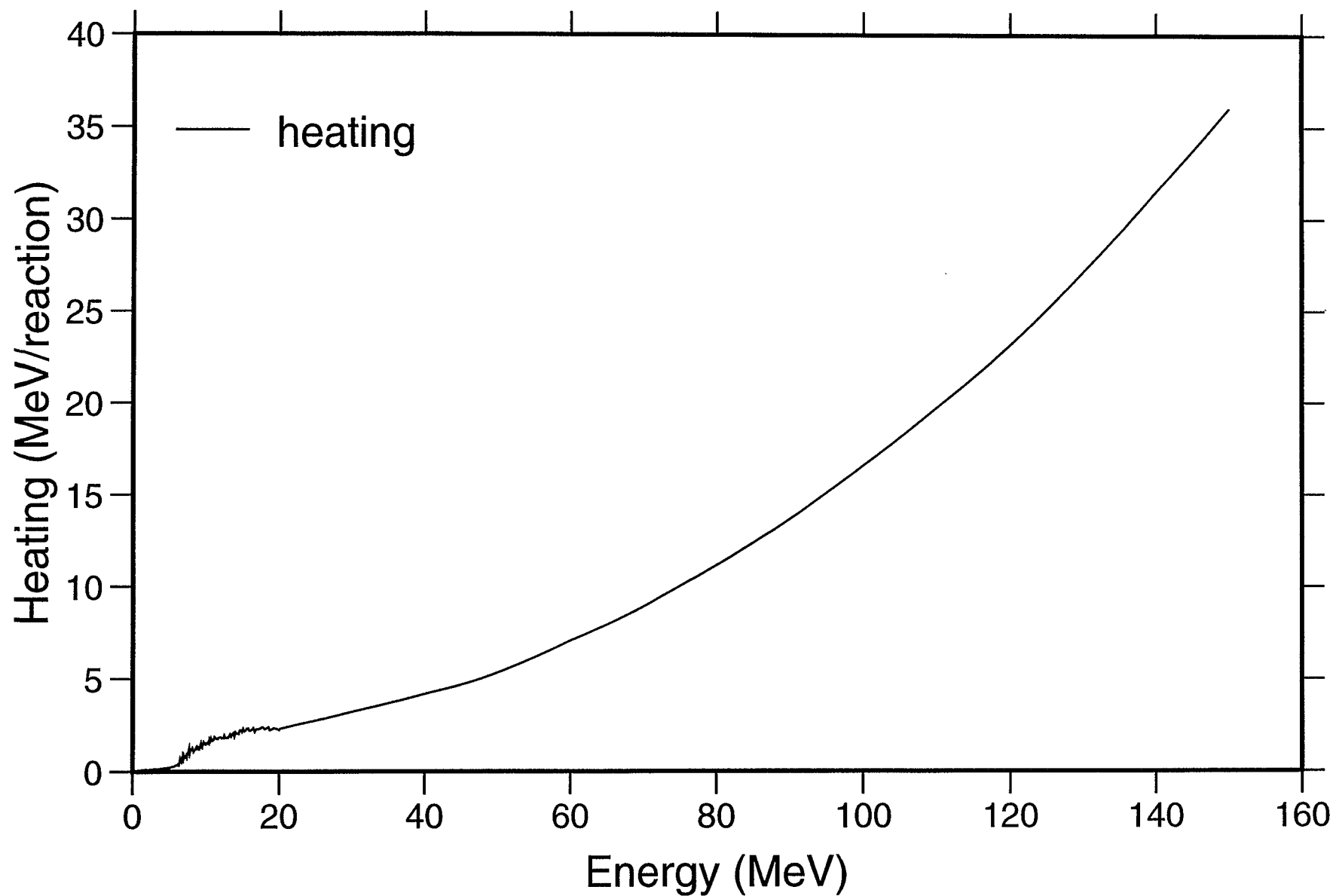


14-SI-28 APT LA150 NJOY 97.18 MCNPX  
angular distribution for elastic



14-SI-28 APT LA150 NJOY 97.18 MCNPX

Heating



14-SI-28 APT LA150 NJOY 97.18 MCNPX

Damage

